Separation Science and Technology
Publication details, including instructions for authors and subscription information:
http://www.informaworld.com/smpp/title~content=t713708471

A modified Donnan-steric-pore model for predicting flux and rejection of dye/NaCl mixture in nanofiltration membranes

A. Wahab Mohammad[a]
[a] Department of Chemical and Process Engineering, Universiti Kebangsaan Malaysia, Selangor, Malaysia

Online publication date: 24 April 2002

To cite this Article Mohammad, A. Wahab(2002) 'A modified Donnan-steric-pore model for predicting flux and rejection of dye/NaCl mixture in nanofiltration membranes', Separation Science and Technology, 37: 5, 1009 — 1029
To link to this Article: DOI: 10.1081/SS-120002238
URL: http://dx.doi.org/10.1081/SS-120002238

SEPARATION SCIENCE AND TECHNOLOGY, 37(5), 1009–1029 (2002)

A MODIFIED DONNAN–STERIC-PORE MODEL FOR PREDICTING FLUX AND REJECTION OF DYE/NaCl MIXTURE IN NANOFILTRATION MEMBRANES

A. Wahab Mohammad*

Department of Chemical and Process Engineering,
Universiti Kebangsaan Malaysia, 43600 UKM Bangi,
Selangor, Malaysia

ABSTRACT

This paper presents a modified Donnan–steric-pore model (DSPM) to predict the rejection of mixture of salts/charged organic in nanofiltration (NF) membranes, based on the extended Nernst–Planck equation with the incorporation of charge and steric effects for the transport of ions inside the membrane, and incorporation of concentration polarization effect for a mixture of charged ions/solutes. With this approach, the permeate flux can be calculated based on the concentration of ions/charged solutes at the membrane surface. The membrane performance was modeled using three parameters, namely: effective pore radius, r_p; effective ratio of membrane thickness to porosity, $\Delta x/A_k$; and the effective charge density, X_d. Comparison of the calculation based on the model with published experimental data shows that the model can predict the tendencies and patterns of rejection and flux reduction

*Fax: (603) 892-96148; E-mail: wahabm@eng.ukm.my

behavior reasonably well for systems containing NaCl–dye–H_2O. Effects on fluxes and NaCl rejections of system variables such as mass transfer film thickness, dye valence, dye diffusivity, and dye/salt concentration ratio were studied using this model. This model can be used as a preliminary tool to assess the rejection capability as well as the flux behavior of NF membranes towards binary solution and mixtures.

Key Words: Nanofiltration; Nernst–Planck equation; Multicomponent; Assessment tools

INTRODUCTION

Nanofiltration (NF) membranes are a relatively new class of membranes, which have properties in between those of ultrafiltration (UF) membranes and reverse-osmosis (RO) membranes. Their separation mechanisms involve both steric (sieving) and electrical (Donnan) effects. This combination allows the NF membranes to be effective for a range of separations of mixtures of small organic solutes (either neutral or charged) and salts (1). One of the main applications in which NF has been used successfully is in the removal of dye compounds from color baths in the textile industry (2,3). This paper will look into the modeling of flux and rejection of multicomponent mixture solutions containing dye and salts.

So far, only two main approaches have been used to model the transport of ionic species through NF membranes. One approach is through the Spiegler–Kedem model (4–7). This black-box approach allows the membranes to be characterized in terms of salt permeability, P_s, and the reflection coefficient σ. This model is, in the first instance, limited to binary salt systems and in the limiting case, to a binary salt system in the presence of a completely rejected organic ion (5,7). One major disadvantage of this model is that the effect of concentration polarization at the membrane surface in multicomponent mixtures could not be quantified properly. Levenstein et al. (5), while using a similar model for mixtures of salts and dyes, used a mass transfer correlation for a single solute and did not account for the effect on the mass transfer due to the presence of multicomponent mixtures of ions and charged solutes at the membrane surface. Thus, permeate fluxes were treated as an independent variable, which was modeled based on the experimental values. In actuality, the permeate fluxes are dependent on the osmotic pressure at the membrane surfaces caused by the multicomponent ions and solutes.

The second approach is based on the extended Nernst–Planck equation. Tsuru et al. (8) first proposed such a model for NF membranes, describing the

MARCEL DEKKER, INC.
270 Madison Avenue, New York, New York 10016

transport of ions in terms of an effective membrane thickness/porosity ratio (m) $\Delta x/A_k$, and an effective membrane charge density (mol m^{-3}) X_d. The model was successful in describing the rejection of mixed salt solutions. In a later work (9), a similar model but with the inclusion of steric effects was used to model the transport of organic electrolytes in the presence of Na^+ and Cl^- ions. In both studies involving multicomponent mixtures, the concentration polarization effect was considered negligible.

In a more recent work, Bowen et al. (10) introduced the Donnan–steric-pore model (DSPM) that was a modified form of the extended Nernst–Planck model. This model takes into account the hindrance effects for diffusion and convections to allow transport of ions/charged solutes within a confined space inside the membranes. This inclusion allows the membranes to be characterized in terms of an effective pore radius, r_p, in addition to $\Delta x/A_k$ and X_d. Subsequent studies (11,12) show that the model can very well predict the rejection performance of single salt solutions. A modified form of the DSPM model was also used successfully to model the performance of an NF membrane in separating the components of a dye/salt solution during a diafiltration process (13). In that study, the concentration polarization effect was taken into account by describing the transport of multicomponent ions and solute in the mass transfer film layer using the extended Nernst–Planck equation. In such a manner, the permeate fluxes were predicted based on the osmotic pressure determined at the membrane interface.

The objective of this paper was to investigate further the capability of the proposed modified DSPM model (13) to predict the separation performance of a multicomponent mixture consisting of a large organic four-valent charged dye with Na^+ and Cl^-. The experimental data of Levenstein et al. (5) have been used as a reference for simulation. The experimental results obtained by Levenstein et al. (5) were compared to the predicted calculations. Then, the effects of several system parameters such as mass transfer film thickness, dye valence, dye diffusivity, and dye/salt concentration ratio with regard to fluxes and rejection of salts were investigated. Results will be presented in terms of characterization of the membrane used as well as prediction of the NaCl rejections and permeate fluxes.

DESCRIPTION OF MODEL

Figure 1 shows the system within which the transport takes place. The bulk components consist of Na^+, Cl^-, and a multivalent dye molecule. For ions/solutes to permeate across the membrane, each ion/solute will move from the bulk solution through the film layer, membrane interface, and inside the membrane. The proposed model takes into account the transport across all the mentioned mediums.

MARCEL DEKKER, INC.
270 Madison Avenue, New York, New York 10016

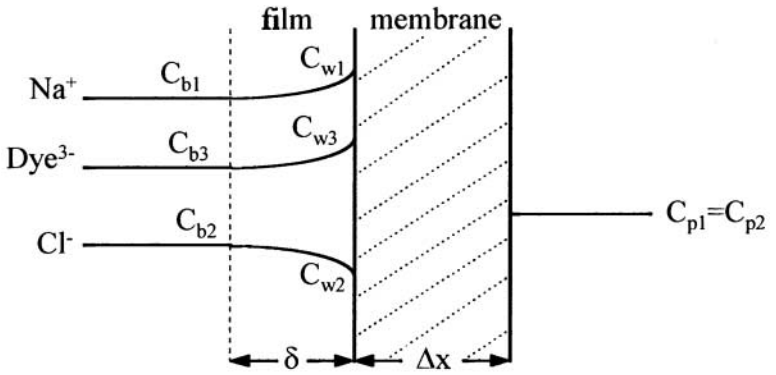

Figure 1. Schematic of the film layer and membrane for three-component system.

Concentration polarization close to the membrane surface is assumed to occur within a boundary film layer of thickness, δ, which is dependent on the mass transfer characteristics of the system. For a system containing charged ions, a mass balance for the film layer yields

$$j_i = -D_{i,\infty}\frac{\mathrm{d}C_i}{\mathrm{d}x} - \frac{z_i F}{RT}C_i D_{i,\infty}\frac{\mathrm{d}\psi_\mathrm{f}}{\mathrm{d}x} + C_i J_\mathrm{v} \tag{1}$$

$D_{i,\infty}$ is the bulk diffusivity of ion i in the solution. The equation can be solved using the boundary conditions at $x = -\delta$, $c = C_\mathrm{bi}$ and at $x = 0, c = C_\mathrm{wi}$.

Similarly, the transport of ions/charged solutes across the membrane will be governed by similar equation based on the extended Nernst–Planck equation.

$$j_i = -D_{i,\mathrm{p}}\frac{\mathrm{d}c_i}{\mathrm{d}x} - \frac{z_i c_i D_{i,\mathrm{p}}}{RT}F\frac{\mathrm{d}\psi}{\mathrm{d}x} + K_{i,\mathrm{c}}c_i V \tag{2}$$

where j_i is the flux of ion i, and the terms on the right hand side represent transport due to diffusion, electric field gradient, and convection, respectively (see Nomenclature for definition of symbols). The hindered nature of diffusion and convection of the ions inside the membrane are accounted for by the terms $K_{i,\mathrm{d}}$ and $K_{i,\mathrm{c}}$. Further details for solution of this equation for transport through NF membranes can be found elsewhere (9,13). Table 1 shows other supporting equations used in this model.

The permeate flux will be calculated as follows

$$J_\mathrm{v} = P_\mathrm{m}(\Delta P - \Delta\pi) \tag{3}$$

Table 1. Equations for the Donnan–Steric-Pore Model (DSPM)

Main Equations:

Concentration gradient:

$$\frac{dc_i}{dx} = \frac{J_v}{D_{i,p}}(K_{i,c}c_i - C_{i,p}) - \frac{z_i c_i}{RT}F\frac{d\psi_m}{dx} \quad (a)$$

Potential gradient:

$$\frac{d\psi_m}{dx} = \frac{\sum_{i=1}^{n}\frac{z_i J_v}{D_{i,p}}(K_{i,c}c_i - C_{i,p})}{\frac{F}{RT}\sum_{i=1}^{n}(z_i^2 c_i)} \quad (b)$$

Donnan–steric partitioning:

$$\left(\frac{\gamma_i c_i}{\gamma_i^0 C_i}\right) = \Phi \exp\left(-\frac{z_i F}{RT}\Delta\psi_D\right) \quad (c)$$

where

Hindrance factors:

$$K_{i,d} = K^{-1}(\lambda,0)K_{i,c} = (2-\Phi)G(\lambda,0) \quad (d)$$

$$D_{i,p} = K_{i,d}D_{i,\infty} \quad (e)$$

Hydrodynamic drag coefficients:

$$K^{-1}(\lambda,0) = 1.0 - 2.30\lambda + 1.154\lambda^2 + 0.224\lambda^3 \quad (f)$$

$$G(\lambda,0) = 1.0 + 0.054\lambda - 0.988\lambda^2 + 0.441\lambda^3 \quad (g)$$

Steric partitioning:

$$\Phi = (1-\lambda)^2 \quad (h)$$

Electroneutrality conditions:

$$\sum_{i=1}^{n} z_i C_i = 0 \quad \sum_{i=1}^{n} z_i c_i = -X_d \quad (i)$$

MARCEL DEKKER, INC. 270 Madison Avenue, New York, New York 10016

where the osmotic pressure difference, $\Delta\pi$, is calculated based on the van't Hoff law (14),

$$\Delta\pi = RT\left(\sum C_{wi} - \sum C_{pi}\right) \tag{4}$$

The van't Hoff model is a rough estimation of the osmotic pressure effect. At higher concentrations, the van't Hoff model will overestimate the osmotic pressure and thus a more accurate model such as the Pitzer model should have been used (2). The Pitzer model includes an osmotic pressure coefficient, ϕ, to indicate deviation from the van't Hoff model. The coefficient ϕ depends on several interaction coefficients, which are available for most salts. However, for larger organic compounds such as the dye considered in this work, determination of ϕ would require further experimental work, which is beyond the scope of this study.

In this model, the transport of the ions/charged solute will be described in terms of only three parameters characteristic of the membrane, namely, r_p, $\Delta x/A_k$, and X_d. By providing these parameters and the operating conditions of the system (concentration, pressure, temperature, and interface boundary film thickness), the model will be able to calculate the rejection of each ion. The flux will also be calculated based on the osmotic pressure at the membrane wall (Eq. (3)). Figure 2 shows the flowchart for the solution of the model. Once the input data are provided, the osmotic pressure, $\Delta\pi$, can be calculated based on the bulk concentrations as well as a guessed permeate concentration. Then the permeate flux, J_v, can be determined based on the pressure driving force. Knowing J_v, Eq. (1) can be solved to obtain the wall concentrations for each solute, C_{wi}. This will be done iteratively until the calculated $\Delta\pi$ is the same as the previously guessed $\Delta\pi$. Eqs. (a)–(i) will then be solved for the transport inside the membrane to obtain the permeate concentration, C_{pi}, for each solute. Again iterative calculations are required until the calculated C_{pi} is the same as the initially guessed C_{pi}. Once C_{pi} is determined, the real rejection, R, can be calculated. For this work, the solute radius of the used dye is larger than the pore radius of the membrane. Thus, the rejection of the dye will be unity. In the film layer, the transport of all three solutes (dye, Na^+, and Cl^-) is taken into account. However, inside the membrane, only the transport of Na^+ and Cl^- is modeled.

MEMBRANES AND SYSTEM PROPERTIES

The data of Levenstein et al. (5) is used to compare the simulation result. In their work, the membrane used was MPF-44 (Membrane Products–Kiryat Weizmann Ltd, Rehovot, Israel). In order to use DSPM model, the membrane has to be characterized in terms of r_p, $\Delta x/A_k$, and X_d. The MPF-44 is a relatively tight NF membrane with glucose rejection of 0.93 at 3.03 MPa. Using this data, Bowen

MARCEL DEKKER, INC.
270 Madison Avenue, New York, New York 10016

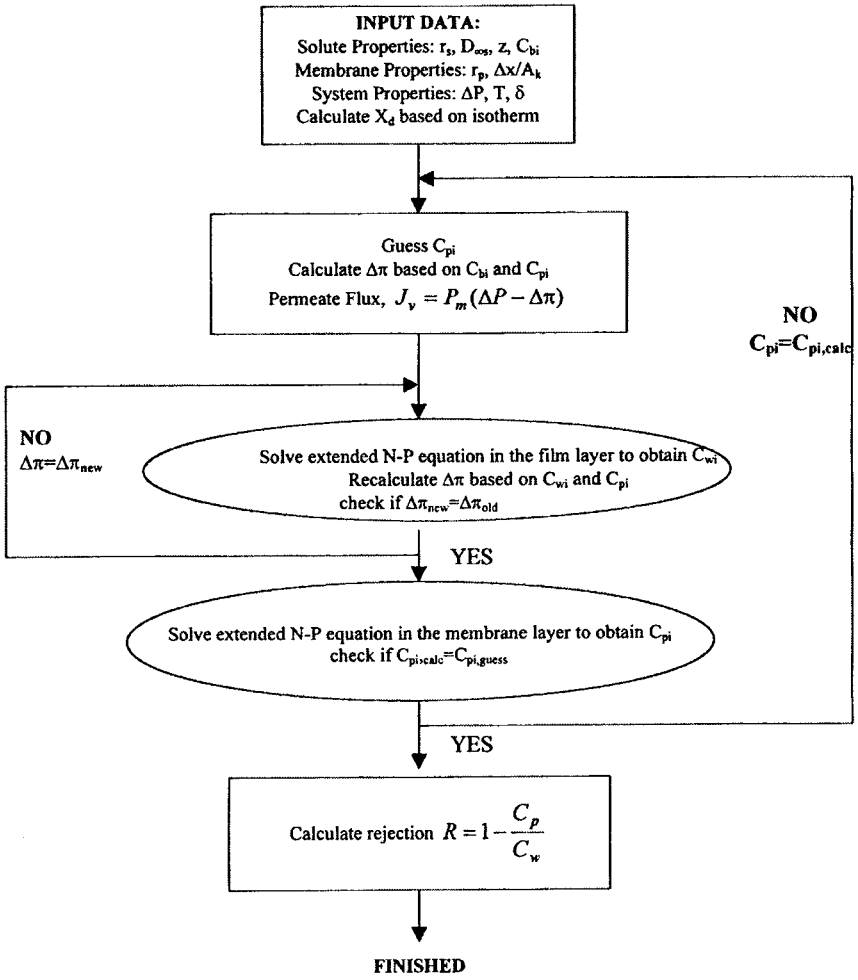

Figure 2. Flowchart for DSPM model for Dye–NaCl–H_2O system.

and Mohammad (15) have approximated r_p of MPF-44 as 0.42 nm. Levenstein et al. (5) reported the pure water permeability, P_m, as 2.58 L hr^{-1} m^{-2} atm^{-1}. From the Hagen–Poiseuille equation (10), P_m can be correlated to r_p and $\Delta x/A_k$ as follows:

$$P_m = \frac{r_p^2}{8\mu(\Delta x/A_k)} \tag{5}$$

Thus, from Eq. (5), $\Delta x/A_k$ is calculated to be 3.48 μm. This value is within the range reported for NF membranes (15).

In order to obtain the isotherm for X_d as a function of C_b, the DSPM model is fitted to the rejection data of NaCl as reported by Levenstein et al. (5). Figure 3 shows the experimental data and the fitted curves for various concentrations of NaCl. The data were fitted very well by using r_p and $\Delta x/A_k$ calculated previously. Figure 4 shows the values of $|X_d|$ obtained as a function of C_b. It can be seen that $|X_d|$ increased as C_b increased, which is similar to the trend reported previously (8,9,13,16). However, in this case the data takes the form of a Langmuir isotherm. The isotherm can be represented as:

$$|X_d| = \frac{1156 C_b}{172.8 + C_b} \tag{6}$$

Table 2 lists the properties of solutes and other required parameters. For Na^+ and Cl^-, the values used were obtained from published data (10). For the dye, the solute radius, r_s, is approximated based on an equation, which correlates r_s of various solutes and their molecular weight, M_w (13). The infinite diffusivity is based on Stokes relationship (10). The boundary film layer, δ, was assumed to be 8.24 μm based on the mass transfer coefficient for the system as reported by Levenstein et al. (5).

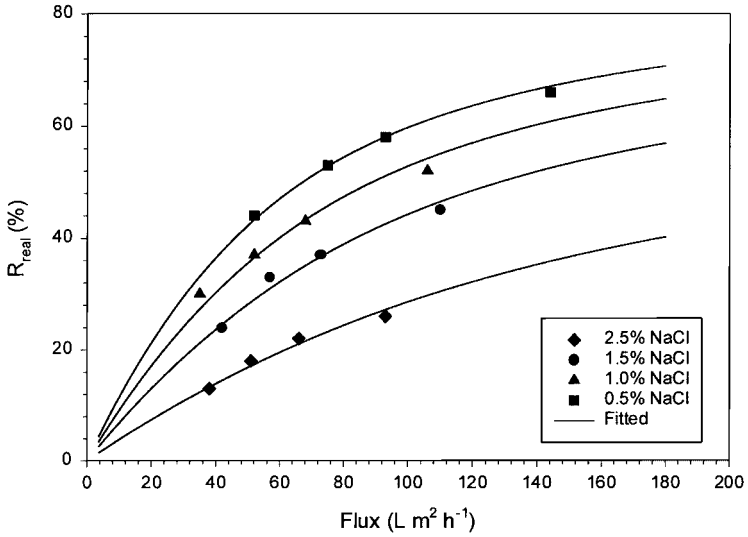

Figure 3. Experimental and fitted data for NaCl rejection in NaCl–H_2O system. Experimental data from Levenstein et al. (5).

MARCEL DEKKER, INC.
270 Madison Avenue, New York, New York 10016

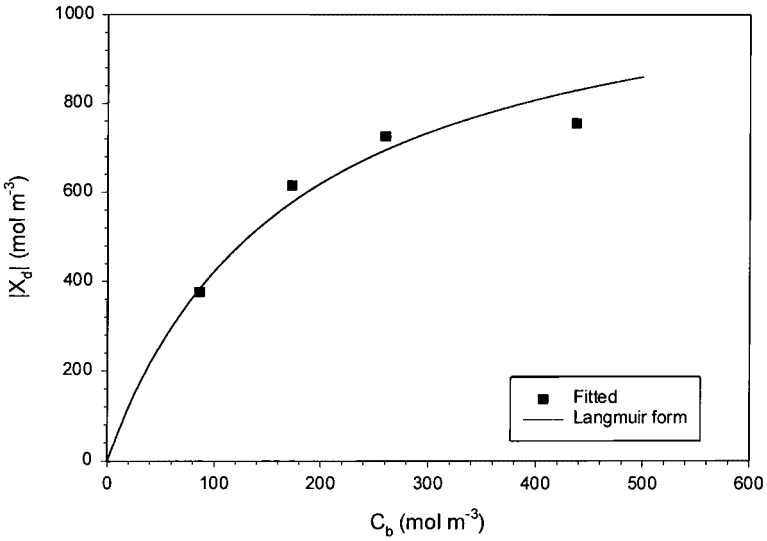

Figure 4. Fitted values of charge density as a function of bulk concentration and the fitted Langmuir isotherm curve.

MODELING DYE–NaCl–H_2O SYSTEM

Table 3 shows the concentrations of salts and dyes used in the experiments by Levenstein et al. (5). In each solution mixture, the NaCl concentration was set 1.2 wt% while the dye concentration varied from 0.13 to 10.7 wt%. The wt% was converted to mol concentration in mol m^{-3} for input into the model. Each solution mixture was permeated at four different applied pressures up to 30.3 bar (30 atm). In modeling the mixture solutions, the charge density, X_d, was taken to be a function of the total concentration of anions in the feed solution, $C_{T,-ve}$, which was equivalent to the concentration of Na^+ ions (13). The C_b in Eq. (6) was replaced by $C_{T,-ve}$ calculated as

$$C_{T,-ve} = C_{Na^+} = 4C_{dye} + C_{Cl^-} \tag{7}$$

Figure 5 shows the plot of permeate fluxes for all four-solution mixtures as a function of ΔP. The 10.7% dye solution as expected has the largest flux reduction compared to other mixtures. There was an anomaly in the experimental data because the highest fluxes obtainable with 0.13 and 1.60 wt% dye were higher than what would be expected from the water permeability data, P_m. On the basis of P_m, at 30 atm the water flux should be about 80 L m^{-2} hr^{-1}. However, the data show that the fluxes in the mentioned cases exceeded 90 L m^{-2} hr^{-1}. Similar

Table 2. Properties of Solutes and Other System Parameters for Input into DSPM Model

Solutes	M_w	r_s (nm)	$D_{\infty s}$ ($m^2\,sec^{-1}$)	z
Na^+	23	0.184	1.33×10^{-9}	+1
Cl^-	35.5	0.121	2.03×10^{-9}	−1
Dye (Procion Red H-E7B)	986	0.70	0.38×10^{-9}	−4
System Properties				
		Film layer thickness = $\delta = 8.24\,\mu m$		
		Maximum Applied Pressure = 30 atm		
		Temperature = 25°C		
Membrane Properties		Pore radius = $r_p = 0.42$ nm		
		Membrane/porosity ratio = $\Delta x/A_k = 3.48\,\mu m$		

Table 3. Concentration of Solution Mixtures Used in Work of Levenstein et al. (5)

Solution Mixture	Weight (%) NaCl (%)	Weight (%) Dye (%)	C_b (NaCl) ($mol\,m^{-3}$)	C_b (dye) ($mol\,m^{-3}$)
1	1.2	0.13	207.48	1.33
2	1.2	1.6	210.62	16.66
3	1.2	5.8	220.13	63.12
4	1.2	10.7	232.37	122.93

behavior was found with the salt permeation fluxes (Fig. 3). The fluxes at higher ΔP were in the region of 90–150 $L\,m^{-2}\,hr^{-1}$. On the basis of Eq. (3), due to the presence of osmotic pressures from NaCl and dye molecules, the permeate fluxes should be lower than the expected water flux. Levenstein et al. (5) did not make any comment on this anomaly. This anomaly may contribute to the differences between the predicted results and the experimental data as will be shown next.

The solid lines in Fig. 5 show the predicted permeate fluxes based on the model calculation. The thick line is the predicted water flux for the membrane based on the membrane permeability, P_m. The sequence of predicted fluxes for the mixture solutions is $J_v(0.13\%) > J_v(2.6\%) > J_v(5.8\%) > J_v(10.7\%)$. Even though the predicted fluxes did not match with the experimental data, the trend shown is very similar. As the dye concentration change from 5.8 to 10.7%, there was a marked reduction in the permeate fluxes, and this pattern of flux reduction was predicted well by the model. The model used in this study assumed that the permeate flux reduction was only due to the osmotic pressure effects of the dye

MARCEL DEKKER, INC.
270 Madison Avenue, New York, New York 10016

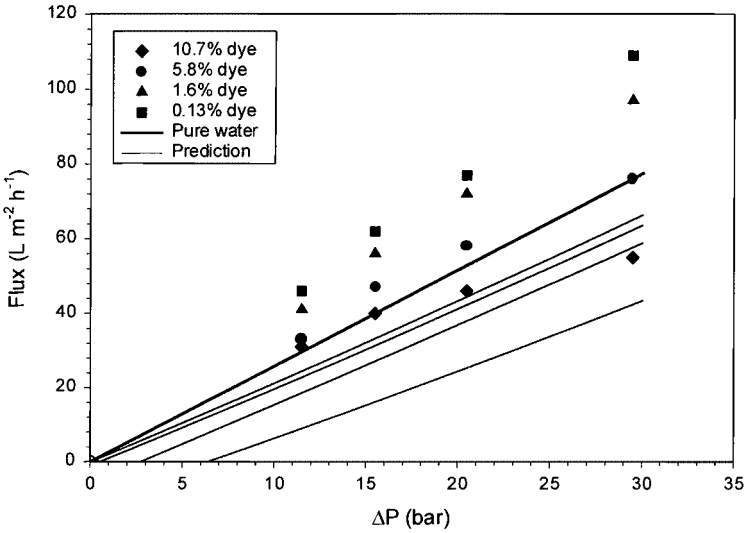

Figure 5. Experimental and predicted fluxes in NaCl–Dye–H_2O system as a function of ΔP. Experimental data from Levenstein et al. (5).

and salt solutes. If the permeate fluxes were to be measured over a longer period of time, other flux reduction mechanisms such as fouling or pore blocking may become important (2). In such cases, the flux equation [Eq. (3)] can be modified by including additional resistance factors due to other flux reduction mechanisms such as adsorption, pore plugging, and fouling. Dal-Cin et al. (17) proposed experimental methods to evaluate quantitatively the relative contribution of these reduction mechanisms.

Figures 6 and 7 show the experimental and predicted rejections of NaCl as functions of ΔP and permeate fluxes, J_v, respectively. The experimental data show that the NaCl rejection increased as ΔP and J_v increased. At higher dye concentrations, the NaCl rejection was observed to be negative. Negative rejection is caused by the presence of multivalent anions at the membrane interface, which due to the enhanced Donnan effect, caused the monovalent Cl^- anions to permeate effectively through the membrane at higher concentration in order to maintain electroneutrality at the interface. Thus, at higher dye concentrations, the rejection of NaCl becomes even more negative. The model was able to predict similar trends of rejections. As shown in Fig. 7, there was a small difference between rejection of 0.13 and 1.60 wt% solution. However, on changing from 1.60 to 5.8 wt%, there was a marked difference in NaCl rejection with the 5.8 wt% solution showing negative

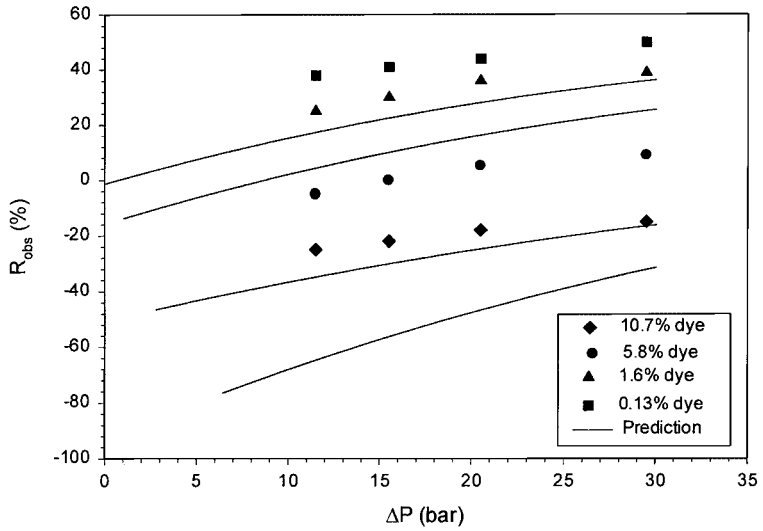

Figure 6. Experimental and predicted NaCl rejection in NaCl–Dye–H_2O system as a function of ΔP. Experimental data from Levenstein et al. (5).

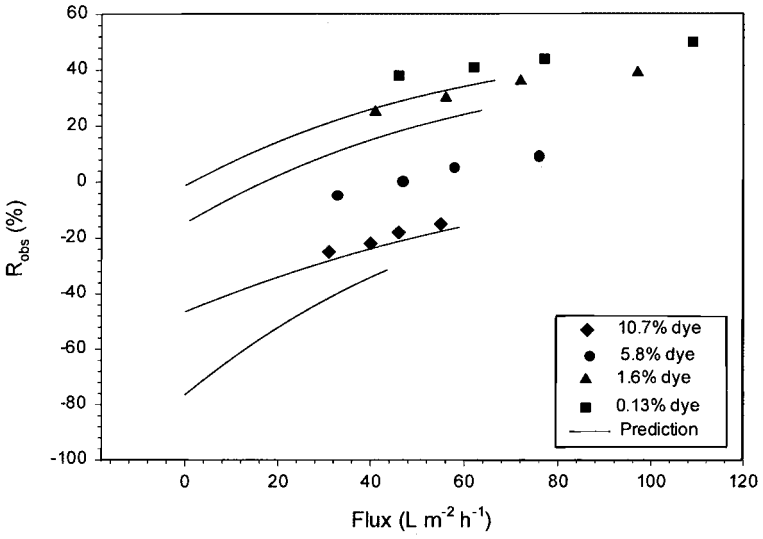

Figure 7. Experimental and predicted NaCl rejection in NaCl–Dye–H_2O system as a function of permeate flux. Experimental data from Levenstein et al. (5).

MARCEL DEKKER, INC.
270 Madison Avenue, New York, New York 10016

rejections. Again, the model was able to predict this trend reasonably well. If not for the previously mentioned anomaly in the experimental data, the agreement between predicted and experimental rejection may be smaller. In addition, it is also possible that due to high concentrations of NaCl and dyes used in the experimental work, the assumption of ideality in developing the model may no longer hold true. The diffusion coefficient used that was based on infinite dilution diffusivity could have changed considerably as well. These shortcomings may be improved/modified if further detailed experimental work is carried out. However, the fact that the tendencies and patterns of rejection and flux reduction can be predicted based on three membrane parameters, which were estimated through water flux and simple salt data, is quite encouraging.

APPLICATION OF THE MODEL

In a previous work (13), the model had been used to predict and optimize the diafiltration process involving a mixed solution of a dye and NaCl. The model was able to show the variation of NaCl rejection during the process, and thus the optimum diafiltration regime could be predicted. The main advantage of this model is that it depends on film layer thickness, δ, and three membrane parameters: r_p, $\Delta x/A_k$, and X_d. The film layer thickness can be estimated based on the mass transfer correlations which is normally in the form of (14):

$$N_{Sh} = \frac{kd_h}{D} = aN_{Re}^{b}N_{Sc}^{0.25} \tag{8}$$

where N_{Sh} is the Sherwood number, N_{Re} the Reynolds number, and N_{Sc} the Schmidt number. The film layer thickness is obtained through the following relation with mass transfer coefficient, k,

$$k = \frac{D}{\delta} \tag{9}$$

The three membrane parameters can be estimated based on the rejection data or molecular weight cut-off (MWCO) provided by membrane manufacturers (15). Once these are available, some assessment on the rejection capability as well as the flux behavior of the membrane towards binary solution and mixtures can be carried out. In the following sections, the effect of mass transfer film thickness, dye valence, dye diffusivity, and dye/salt concentration ratio with regard to fluxes and rejections were studied. In analyzing these effects, the reference data used was the 5.8% dye solution. In each case, only the studied variable is varied while other parameters and variables were the same as for the 5.8% dye case.

MARCEL DEKKER, INC.
270 Madison Avenue, New York, New York 10016

Effect of Mass Transfer Film Thickness, δ

The mass transfer film thickness, δ, as shown in Eq. (8), depends on the type of flow of the system. A large Reynolds number, N_{Re}, means that the mass transfer coefficient, k, is large as well. This means that δ will be smaller since δ is inversely proportional to k. For the reference case, which was based on the experimental conditions of Levenstein et al. (5), δ was calculated to be 8.24 μm based on N_{Re} of 5500. For this comparison, δ is reduced and increased by a factor of 5. Thus, δ was simulated between 1.65 and 41.2 μm, which corresponded to N_{Re} of 34,600 (turbulent flow) and 874 (laminar flow), respectively.

Figure 8a–b shows the calculated results. The results show that the fluxes increase slightly when δ is reduced (N_{Re} increased). However, the reduction in fluxes is higher when δ is increased to 41.2 μm (N_{Re} of 824). This is expected since turbulent flow will induce less concentration polarization at the membrane surface. The calculated rejections show less negative rejection of NaCl at lower δ and much more negative rejection at higher δ. This is due to the fact that at higher δ, (laminar flow) more dye molecules are accumulated at the membrane surface. This will enhance the Donnan effect, thus causing more NaCl to be negatively rejected. A similar phenomenon was observed in the experimental data (Fig. 6) whereby higher bulk concentration of dye induced more negative rejection of NaCl.

Effect of Dye Valence

The dye used in Levenstein et al.'s work (5) had a valence of -4. In this study, the valence was varied from -2 to -6. Figure 9a–b shows the calculated fluxes and NaCl rejections. There is no much effect of valency on the fluxes obtained. However, there are significant differences in the NaCl rejections. Again, higher valances will enhance the Donnan effect, thus causing more NaCl to permeate. On the basis of calculated results, a difference of -2 in the valence will correspond to about 20–30% difference in rejections with more negative rejections at higher valences.

Effect of Dye Diffusivity

For this case the diffusivity, D_∞, of the dye is increased and decreased by a factor of 5. The reference case used a diffusivity of $0.38 \times 10^{-9}\ \mathrm{m^2\ sec^{-1}}$. The diffusivity is related inversely to the solute radius, r_s, by the Stokes relationship (10). Thus by changing D_∞, the r_s will change as well. Since for this study, the dye was assumed to be completely rejected, the change in D_∞ and thereby r_s will

MARCEL DEKKER, INC.
270 Madison Avenue, New York, New York 10016

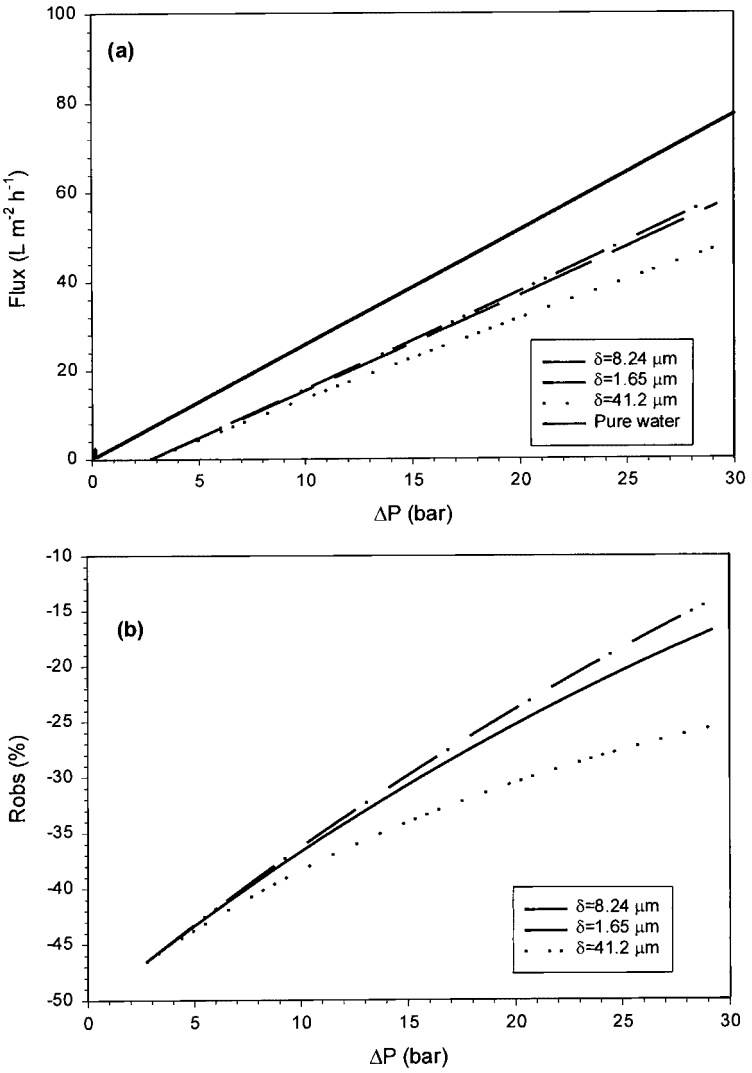

Figure 8. Effect of varying film layer thickness, δ, on (a) permeate flux, and (b) observed rejection of NaCl.

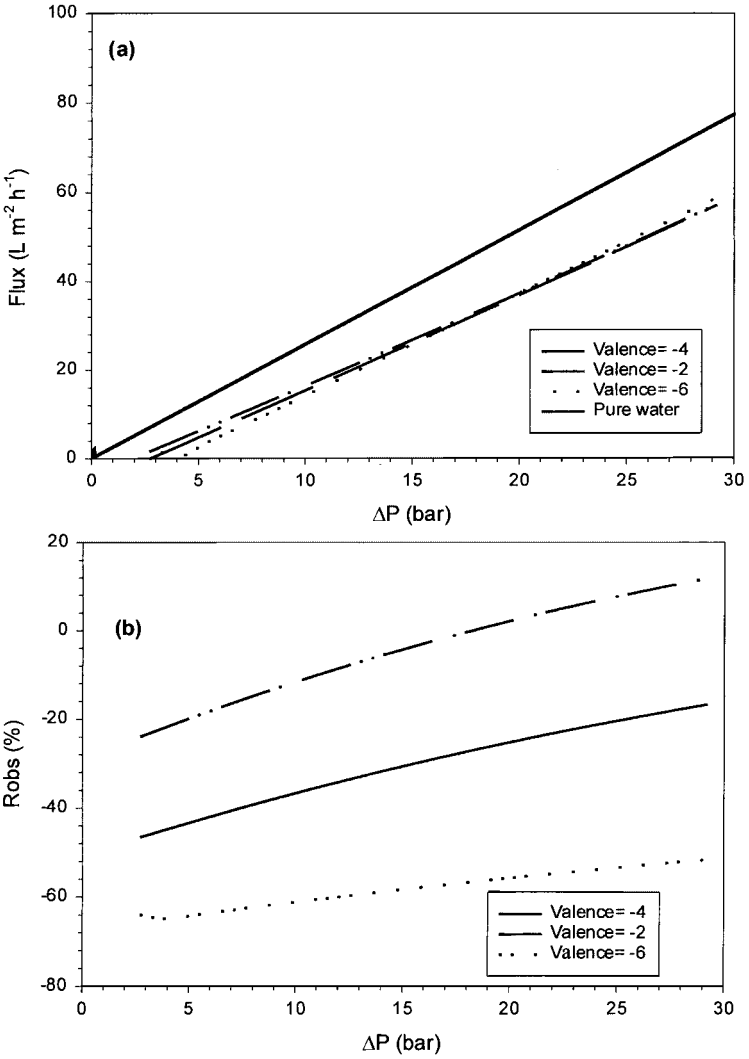

Figure 9. Effect of varying dye valence on (a) permeate flux, and (b) observed rejection of NaCl.

be assumed to have no effect on dye rejection. Figure 10a–b shows the results for this case. The results show that higher D_∞ will cause an increase in fluxes and less negative NaCl rejection. Again this is due to the fact that higher D_∞ means that less dye is accumulated at the membrane surface, and this will improve the fluxes and induce less Donnan effect on the permeated NaCl.

MARCEL DEKKER, INC.
270 Madison Avenue, New York, New York 10016

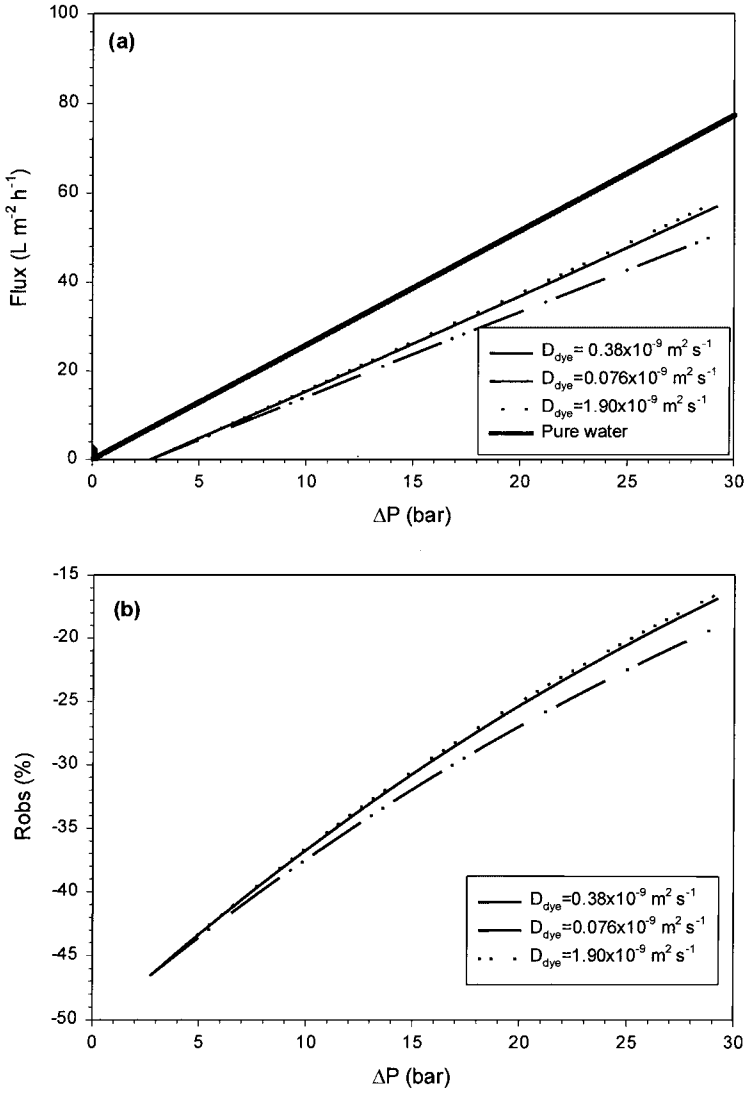

Figure 10. Effect of varying dye diffusivity, $D_{\infty,\text{dye}}$ on (a) permeate flux, and (b) observed rejection of NaCl.

MARCEL DEKKER, INC.
270 Madison Avenue, New York, New York 10016

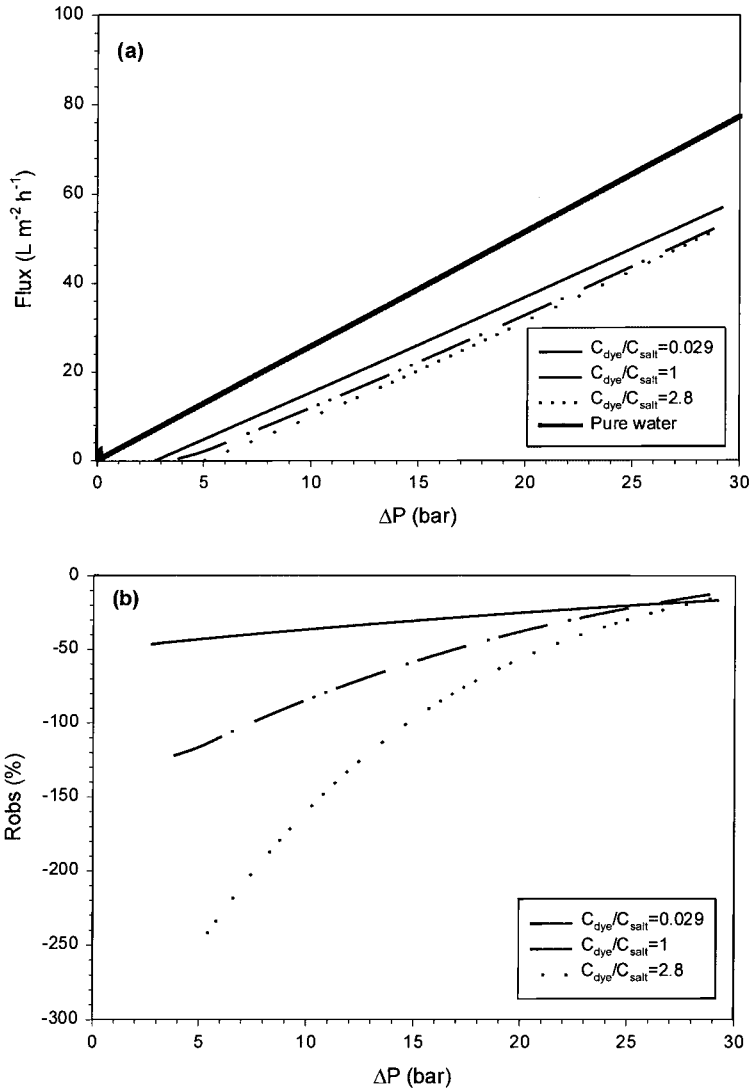

Figure 11. Effect of varying concentration ratio of dye/NaCl on (a) permeate flux, and (b) observed rejection of NaCl.

MARCEL DEKKER, INC.
270 Madison Avenue, New York, New York 10016

Effect of Dye/Salt Concentration Ratio

For the last case, the ratio of dye to NaCl concentration is varied. The reference case had a dye/NaCl ratio of 0.29 with NaCl concentration at 220.1 mol m^{-3} and dye concentration at 63.12 mol m^{-3}. For this simulated case, the dye concentration remained constant while the NaCl concentration was reduced to 63.12 and 22.50 mol m^{-3} giving ratios of 1 and 2.8, respectively.

Figure 11a–b presents the calculated result. Increasing the ratio (by reducing NaCl concentration) results in a slight reduction in fluxes but quite a significant difference in rejection especially at lower ΔP. This phenomenon can be attributed to the varying effect of transport mechanisms (diffusion, electromigration, and convection) in addition to the Donnan effect at the membrane interface (15). Similar findings have been observed with multi-component salt systems containing Na^+, Cl^-, and SO_4^{2-} (16).

CONCLUSIONS

The DSPM model based on the extended Nernst–Planck equation used in this work is very useful in predicting and explaining the pattern of rejection in mixture of salts/charged solutes in NF membranes. The model was described in terms of only three membrane parameters and a mass transfer film layer thickness. Furthermore by incorporating the concentration polarization effect at the membrane surface, the permeate flux was also calculated. Comparison of the model calculation with published experimental data shows that the model can predict the tendencies and patterns of rejection and flux reduction behavior reasonably well for systems containing NaCl–dye–H_2O. The model can be used as a preliminary tool to assess the rejection capability as well as the flux behavior of NF membranes in binary solution and mixtures. Simulation results show that the mass transfer film layer thickness, dye valence, dye diffusivity, and dye/salt ratio affect the rejections and fluxes of the system in varying manners.

NOMENCLATURE

c_i	concentration in membrane (mol m^{-3})
$C_{i,b}$	concentration in the bulk solution (mol m^{-3})
$C_{i,p}$	concentration in permeate (mol m^{-3})
$D_{i,p}$	hindered diffusivity (m^2 sec^{-1})
$D_{i,\infty}$	bulk diffusivity (m^2 sec^{-1})
F	Faraday constant (C mol^{-1})
j_i	ion flux (based on membrane area) (mol m^{-2} sec^{-1})

MARCEL DEKKER, INC.
270 Madison Avenue, New York, New York 10016

$K_{i,c}$	hindrance factor for convection
$K_{i,d}$	hindrance factor for diffusion
N_{Re}	Reynolds number
N_{Sc}	Schmidt number
N_{Sh}	Sherwood number
r_p	effective pore radius (m)
R	gas constant ($J\,mol^{-1}\,K^{-1}$)
T	absolute temperature (K)
x	distance normal to membrane (m)
Δx	effective membrane thickness (m)
X_d	effective membrane charge ($mol\,m^{-3}$)
z_i	valence of ion
δ	thickness of film layer (m)
$\Delta\psi$	potential difference (V)

ACKNOWLEDGMENTS

The author would like to thank the Ministry of Science and Technology, Malaysia for financial support through IRPA Grant 09-02-02-0067.

REFERENCES

1. Raman, L.P.; Cheryan, M.; Rajagopalan, N. Consider Nanofiltration for Membrane Separations. Chem. Eng. Prog. **1994**, *90*, 68–74.
2. van der Bruggen, B.; Daems, D.; Wilms, D.; Vandecasteele, C. Mechanisms of Retention and Flux Decline for the Nanofiltration of Dye Baths from the Textile Industry. J. Membr. Sci. **2001**, *22–23*, 519–528.
3. PCI-Memtech. Membranes Treat Coloured Water. Membr. Technol. **2001**, *2001* (35), 10.
4. Schirg, P.; Widmer, F. Characterisation of Nanofiltration Membranes for the Separation of Aqueous Dye–Salt Solutions. Desalination **1992**, *89*, 89–107.
5. Levenstein, R.; Hasson, D.; Semiat, R. Utilisation of the Donnan Effect for Improving Electrolyte Separation with Nanofiltration Membranes. J. Membr. Sci. **1996**, *116*, 77–92.
6. Xu, X.; Spencer, H.G. Dye–Salt Separations by Nanofiltration Using Weak Acid Polyelectrolyte Membranes. Desalination **1997**, *114*, 129–137.
7. Perry, M.; Linder, C. Intermediate RO UF Membranes for Concentrating and Desalting of Low Molecular Weight Organic Solutes. Desalination **1989**, *71*, 233–245.

MARCEL DEKKER, INC.
270 Madison Avenue, New York, New York 10016

8. Tsuru, T.; Nakao, S.; Kimura, S. Calculation of Ion Rejection by Extended Nernst–Planck Equation with Charged Reverse Osmosis Membranes for Single and Mixed Electrolyte Solutions. J. Chem. Eng. Jpn **1991**, *24*, 511–517.
9. Wang, X.L.; Tsuru, T.; Togoh, M.; Nakao, S.; Kimura, S. The Electrostatic and Steric-Hindrance Model for the Transport of Charged Solutes Through Nanofiltration Membranes. J. Membr. Sci. **1997**, *135*, 19–32.
10. Bowen, W.R.; Mohammad, A.W.; Hilal, N. Characterization of Nanofiltration Membranes for Predictive Purposes—Use of Salts, Uncharged Solutes, and Atomic Force Microscopy. J. Membr. Sci. **1997**, *126*, 91–105.
11. Schaep, J.; Vandecasteele, C.; Mohammad, A.W.; Bowen, W.R. Evaluation of the Salt Retention of Nanofiltration Membranes Using the Donnan and Steric Partitioning Model. Sep. Sci. Technol. **1999**, *34* (15), 3009–3030.
12. Schaep, J.; Vandecasteele, C.; Mohammad, A.W.; Bowen, W.R. Modelling the Retention of Ionic Components for Different Nanofiltration Membranes. Sep. Purif. Technol. **2001**, *22–23* (1–3), 169–179.
13. Bowen, W.R.; Mohammad, A.W. Diafiltration of Dye/Salt Solution by Nanofiltration: Process Prediction and Optimisation. AIChE **1998**, *44*, 1799–1812.
14. Mulder, M. Transport in Membranes. In *Basic Principles of Membrane Technology*; Kluwer: Dordrecht, 1991; 149–159.
15. Bowen, W.R.; Mohammad, A.W. Characterisation and Prediction of Nanofiltration Membrane Performance—A General Assessment. Trans. IChemE **1998**, *76A*, 885–893.
16. Bowen, W.R.; Mukhtar, H. Characterisation and Prediction of Separation Performance of Nanofiltration Membranes. J. Membr. Sci. **1996**, *112*, 263–274.
17. Dal-Cin, M.M.; McLellan, F.; Striez, C.N.; Tan, C.M.; Tweddle, T.A.; Kumar, A. Membrane Performance with a Pulp Mill Effluent: Relative Contributions of Fouling Mechanisms. J. Membr. Sci. **1996**, *120*, 273–285.

Received May 2001
Revised August 2001

Request Permission or Order Reprints Instantly!